Moment actuator influence function for flat circular deformable mirrors

Pravin K. Mehta
Hughes Danbury Optical Systems, Inc.
M S 803
100 Wooster Heights Road
Danbury, Connecticut 06810-7589

Abstract. In some applications, moment actuators provide a competitive alternative approach to the conventional piston type of actuators. A piezoelectric or similar device placed between two posts on the back surface of a deformable mirror constitutes one type of moment actuator. A closed form solution of the biharmonic equation of Kirchhoff's thin plate theory is obtained by the classical method of boundary value problems of linear elastomechanics and presented in this paper for the influence function of an arbitrarily located and oriented moment actuator of the above type on the back of a flat circular deformable mirror. The solution covers both radial and tangential moments. The results clearly show their global character in contrast to those for the piston type actuators with high stiffness. An application of these functions to the design of a 30-actuator circular deformable mirror with moment actuators, related hardware, and test results has been reported elsewhere.

Subject terms: adaptive optical components; moment actuators; influence functions; closed form solutions.

Optical Engineering 29(10), 1213-1222 (October 1990).

CONTENTS

1. INTRODUCTION

Two papers originally were planned on the development of a flat circular deformable mirror with diametral arrays of radial moment actuators. This first paper deals with the development of a cost-effective analytical tool required for configurational trade-offs leading to a near-optimum deformable mirror concept for the correction of specified aberrations. Its application to a real mirror development, hardware, correlation between test and analysis, etc., were to be included in the second paper, which has been scrapped due to customer's disapproval for publication. However, the information is available in an unclassified final report[1] on the project.

The influence function of an actuator in a deformable mirror is required to determine its capability of wavefront or aberration correction, which is usually accomplished by determining the optimum set of actuator actions (force, displacement, moment, or voltage, etc.) that yields a minimum residual wavefront error. A moment actuator is placed parallel to the mirror between two end posts, in contrast to a piston type force or displacement actuator, which is placed perpendicular to the mirror, as shown schematically in Fig. 1. The actuator generates two equal and opposite forces at its two ends, and in the case of the moment actuator, these forces create two equal and opposite bending moments on the mirror at the post locations. Accordingly, our objective is to derive an influence function for unit bending moments M_A and M_B at arbitrary post locations A and B at the ends of a moment actuator, as shown in Fig. 2. We define the mathematical notation in Table I before proceeding with the derivation.

2. SOLUTION APPROACH

The solution of the biharmonic differential equation

$$\nabla^2\nabla^2 w = -a^4\frac{p(\rho,\phi)}{D}\,, \tag{1}$$

$$\nabla^2 = \frac{\partial}{\partial\rho^2} + \frac{1}{\rho}\frac{\partial}{\partial\rho} + \frac{1}{\rho^2}\frac{\partial}{\partial\phi^2}\,, \tag{2}$$

for the bending of a thin, flat, circular plate is first obtained for a concentrated transverse force P_c applied at a radial distance c from the center, as shown in Fig. 3(a). This solution is then

Invited paper AC-109 received March 7, 1990; revised manuscript received July 13, 1990; accepted for publication July 20, 1990.

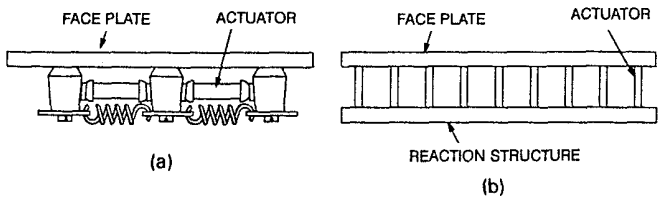

Fig. 1. Two different actuation approaches for deformable mirrors. (a) Deformable mirror with moment actuators parallel to the mirror and/or perpendicular to the optical axis. (b) Deformable mirror with piston actuators parallel to the optical axis and/or normal to the mirror.

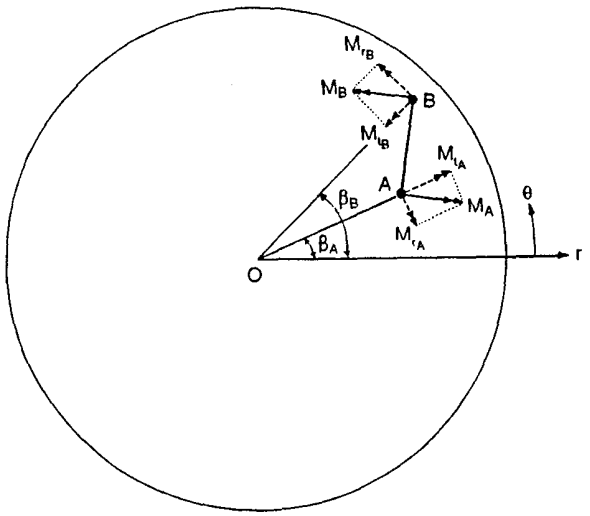

Fig. 2. Arbitrary placement of a moment actuator and related notation.

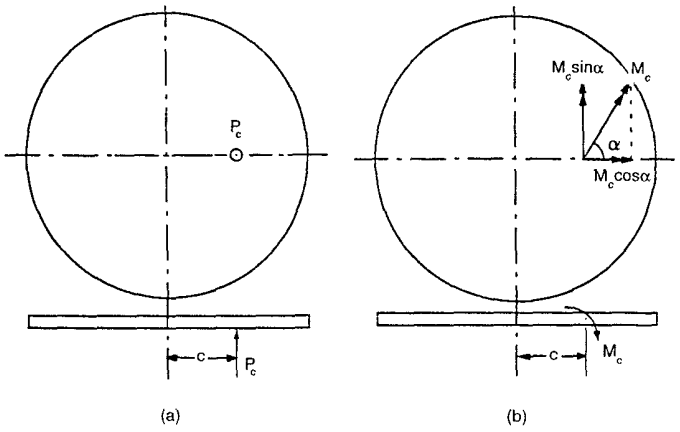

Fig. 3. Solution for a single concentrated force P_c forms the basis of that for a single moment M_c at $r = c$.

utilized to obtain a solution for an arbitrarily oriented bending moment M_c at the same location, as shown in Fig. 3(b). This can be accomplished by superposing the solutions for two equal and opposite forces separated by a small distance e, as shown in Fig. 4, and taking the limit as $e \rightarrow 0$ such that $P_c e = M_c$.

Let $f(c)$ represent any of the many functions of c that may occur in the solution for the concentrated force P_c acting at $r = c$ and $\theta = 0$. The deflection function will then contain

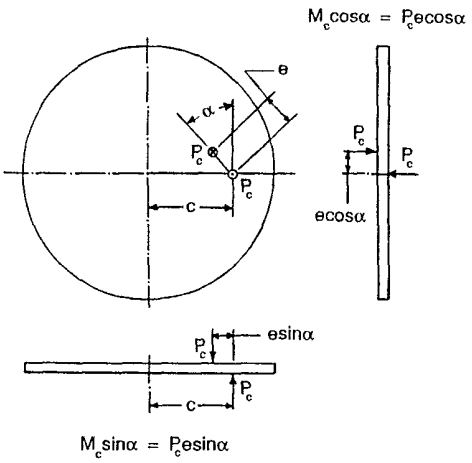

Fig. 4. Superposition of two equal and opposite forces P_c a small distance e apart yields moment M_c in the limit.

terms involving the product $P_c f(c)$. Superposing the case of two equal and opposite forces P_c separated by a small distance e, the resultant deflection function will contain terms such as

$$P_c[f(c) - f(c - e\sin\alpha)] ,$$

$$P_c f(c)\left\{\cos n\left[\theta + \left(\frac{e}{c}\right)\cos\alpha\right] - \cos n\theta\right\} ,$$

for radial and tangential components of the bending moment, respectively. These terms may be respectively rewritten as

$$P_c e\sin\alpha \frac{f(c) - f(c - e\sin\alpha)}{e\sin\alpha}\cos n\theta ,$$

$$\frac{P_c e}{c}\cos\alpha f(c)\frac{\cos n[\theta + (e/c)\cos\alpha] - \cos n\theta}{(e/c)\cos\alpha} .$$

Taking the limits $e \rightarrow 0$ ($c \neq 0$) and replacing $P_c e$ by M_c, these terms respectively reduce to

$$M_c\sin\alpha \frac{df(c)}{dc}\cos n\theta ,$$

$$M_c\cos\alpha \frac{f(c)}{c}\frac{d(\cos n\theta)}{d\theta} .$$

Since $c/a = \rho_c$, it follows that the solution for the applied moment M_c can be derived from that for the applied force P_c by making the following substitutions for the radial and tangential moments, respectively:

$$\frac{M_c\sin\alpha}{a}\frac{df(\rho_c)}{d\rho_c}\cos n\theta \rightarrow P_c f(\rho_c)\cos n\theta , \quad (3)$$

$$\frac{-M_c\cos\alpha}{a}\frac{nf(\rho_c)}{\rho_c}\sin n\theta \rightarrow P_c f(\rho_c)\cos n\theta . \quad (4)$$

If the actuator force or moments are applied at $r = c$ and $\theta = \beta$, then θ in Eqs. (3) and (4) should be replaced by $\phi = \theta - \beta$. The case of $c = 0$ will be treated separately later.

TABLE I. Notation used in the equations.

a = Mirror outer radius
c = Radial location of the applied load
e = Infinitesimal distance
n = Harmonic Index
p = Applied pressure = p(r,θ)
r = Radial coordinate
s = Support circle radius (3-point support)
w = Deflection

D = Mirror flexural rigidity
M_c = Arbitrary bending moment at r = c
M_o = Arbitrary bending moment at r = 0
M_r = Radial bending moment
M_t = Tangential bending moment
M_{rt} = Torsional moment
P_c = Displacement actuator force at r = c
Q_r = Radial shear force
Q_t = Tangential shear force
V_r = Boundary reaction force

α = Orientation angle of the arbitrary bending moment vector M_c at r = c
β = Angular coordinate of an actuator post
θ = Angular coordinate
φ = θ - β = Transformed angular coordinate
ν = Poisson's ratio
ρ = Normalized radial coordinate = r /a
ρ_c = Normalized actuator post radius = c /a
ρ_s = Normalized mirror support radius = s /a

Subscripts :

A = Quantities at actuator post A
B = Quantities at actuator post B
0 = Quantities at r = 0 (center)
c = Quantities at r = c
h = Homogeneous
n = Non-negative integer
r = Radial
s = Quantities at r = s
t = Tangential

Diacritical Marks :

~ = Tilde over symbols to distinguish the outer region (r ≥ c) quantities from those of the inner region (r ≤ c), Figure 3(a).

2.1. General solution

Since there is no applied pressure, the general solution of Eq. (2) consists only of its homogeneous solution, given by[2]

$$w = \sum_{n=0}^{\infty} w_n \cos n\phi \ , \tag{5}$$

where

$$w_0 = A_0\rho^0 + B_0\rho^2 + C_0\ln\rho + D_0\rho^2\ln\rho \ , \tag{6}$$

$$w_1 = A_1\rho^1 + B_1\rho^3 + C_1\rho^{-1} + D_1\rho\ln\rho \ , \tag{7}$$

$$w_n = A_n\rho^n + B_n\rho^{n+2} + C_n\rho^{-n} + D_n\rho^{-(n-2)} \ . \tag{8}$$

A_n, B_n, C_n, and D_n ($n \geq 0$) are constants of integration, and Eq. (8) is applicable for all $n \geq 2$. Dividing the mirror into two concentric circular regions by the dotted circle of load radius c as shown in Fig. 3(a), Eq. (5) can be applied to each region by using two different sets of integration constants. The constants for the outer region ($\rho \geq \rho_c$) are distinguished from those of the inner region ($\rho \leq \rho_c$) by a tilde over each quantity. Thus, similar to Eq. (5), we may write

$$\tilde{w} = \sum_{n=0}^{\infty} \tilde{w}_n \cos n\phi \ , \tag{9}$$

for the outer region ($\rho \geq \rho_c$), where

$$\tilde{w}_0 = \tilde{A}_0\rho^0 + \tilde{B}_0\rho^2 + \tilde{C}_0\ln\rho + \tilde{D}_0\rho^2\ln\rho \ , \tag{10}$$

$$\tilde{w}_1 = \tilde{A}_1\rho^1 + \tilde{B}_1\rho^3 + \tilde{C}_1\rho^{-1} + \tilde{D}_1\rho\ln\rho \ , \tag{11}$$

$$\tilde{w}_n = \tilde{A}_n\rho^n + \tilde{B}_n\rho^{n+2} + \tilde{C}_n\rho^{-n} + \tilde{D}_n\rho^{-(n-2)} \ . \tag{12}$$

Equation (12) is applicable for all $n \geq 2$.

3. CONSTANTS OF INTEGRATION

The constants of integration for the two regions are related by the equations of continuity and shear force balance at the loading circle. We first use these equations to express the constants of the inner region in terms of those of the outer region. The boundary conditions are then used to determine the constants of the outer region.

3.1. Equations of continuity

For continuity at $\rho = \rho_c$, we have for all values of $n \geq 0$,

$$w_n = \tilde{w}_n \ , \quad \frac{dw_n}{d\rho} = \frac{d\tilde{w}_n}{d\rho} \ , \quad \frac{d^2w_n}{d\rho^2} = \frac{d^2\tilde{w}_n}{d\rho^2} \ . \tag{13}$$

Substitution of Eqs. (6) through (8) for w_n and Eqs. (10) through (12) for $\tilde{w}_n$ into Eqs. (13) yields, for every n, three of the four required equations; the fourth equation is obtained later by considering the balance of shear force at the loading circle.

For $n = 0$,

$$A_0 + B_0\rho_c^2 + C_0\ln\rho_c + D_0\rho_c^2\ln\rho_c = \tilde{A}_0 + \tilde{B}_0\rho_c^2 + \tilde{C}_0\ln\rho_c + \tilde{D}_0\rho_c^2\ln\rho_c \ , \tag{14}$$

$$2B_0\rho_c + \frac{C_0}{\rho_c} + D_0\rho_c(1 + 2\ln\rho_c)$$

$$= 2\tilde{B}_0\rho_c + \frac{\tilde{C}_0}{\rho_c} + \tilde{D}_0\rho_c(1 + 2\ln\rho_c) , \quad (15)$$

$$2B_0 - \frac{C_0}{\rho_c^2} + D_0(3 + 2\ln\rho_c)$$

$$= 2\tilde{B}_0 - \frac{\tilde{C}_0}{\rho_c^2} + \tilde{D}_0(3 + 2\ln\rho_c) . \quad (16)$$

For $n = 1$,

$$A_1\rho_c + B_1\rho_c^3 + \frac{C_1}{\rho_c} + D_1\rho_c\ln\rho_c = \tilde{A}_1\rho_c + \tilde{B}_1\rho_c^3 + \frac{\tilde{C}_1}{\rho_c} + \tilde{D}_1\rho_c\ln\rho_c , \quad (17)$$

$$A_1 + 3B_1\rho_c^2 - \frac{C_1}{\rho_c^2} + D_1\rho_c(1 + \ln\rho_c)$$

$$= \tilde{A}_1 + 3\tilde{B}_1\rho_c^2 - \frac{\tilde{C}_1}{\rho_c^2} + \tilde{D}_1\rho_c(1 + \ln\rho_c) , \quad (18)$$

$$6B_1\rho_c + \frac{2C_1}{\rho_c^3} + \frac{D_1}{\rho_c} = 6\tilde{B}_1\rho_c + \frac{2\tilde{C}_1}{\rho_c^3} + \frac{\tilde{D}_1}{\rho_c} . \quad (19)$$

For $n \geq 2$,

$$A_n\rho_c^n + B_n\rho_c^{n+2} + C_n\rho_c^{-n} + D_n\rho_c^{2-n}$$

$$= \tilde{A}_n\rho_c^n + \tilde{B}_n\rho_c^{n+2} + \tilde{C}_n\rho_c^{-n} + \tilde{D}_n\rho_c^{2-n} , \quad (20)$$

$$(A_n - \tilde{A}_n)n\rho_c^{n-1} + (B_n - \tilde{B}_n)(n + 2)\rho_c^{n+1}$$

$$- (C_n - \tilde{C}_n)n\rho_c^{-(n+1)} - (D_n - \tilde{D}_n)(n - 2)\rho_c^{1-n} = 0 , \quad (21)$$

$$(A_n - \tilde{A}_n)n(n - 1)\rho_c^{n-2} + (B_n - \tilde{B}_n)(n + 1)(n + 2)\rho_c^n$$

$$+ (C_n - \tilde{C}_n)n(n + 1)\rho_c^{-(n+2)}$$

$$+ (D_n - \tilde{D}_n)(n - 1)(n - 2)\rho_c^{-n} = 0 . \quad (22)$$

3.2. Shear force balance

The shear force is continuous everywhere except at the point of loading, where it has a discontinuity due to the concentrated load P_c. Representing this load by a Fourier series,[2] the requirement of shear force balance at $\rho = \rho_c$ may be expressed as

$$\left[Q_{r_n} - \tilde{Q}_{r_n}\right]_{\rho=\rho_c} = \frac{P_c}{\rho_c\pi a}\left(\frac{1}{2} + \sum_{n=1}^{\infty}\cos n\phi\right) , \quad (23)$$

where the shear force Q_{r_n} is given by

$$Q_{r_n} = -\frac{D}{a^3}\frac{\partial}{\partial\rho}(\nabla^2 w_n) . \quad (24)$$

Substituting for w_n from Eqs. (6), (7), and (8) into Eq. (24), we have

$$Q_{r_0} = -\frac{4D}{a^3}\frac{D_0}{\rho_c} \quad (25)$$

$$Q_{r_1} = -\frac{2D}{a^3}\left(4B_1 - \frac{D_1}{\rho_c^2}\right)\cos\phi , \quad (26)$$

$$\frac{Q_{r_n}}{(D/a^3)\cos n\phi} = -[4B_n n(n + 1)\rho_c^{n-1} + D_n n(n - 1)\rho_c^{-(n+1)}] , \quad (27)$$

where Eq. (27) is applicable for all $n \geq 2$. Using Eqs. (25) through (27) and similar ones with tildes over the symbols for the outer region, we obtain from Eq. (23) the remaining equations for the determination of the inner region constants in terms of those of the outer region:

$$8(\tilde{D}_0 - D_0) = \frac{P_c a^2}{\pi D} , \quad (28)$$

$$8(\tilde{B}_1 - B_1) - \frac{2(\tilde{D}_1 - D_1)}{\rho_c^2} = \frac{P_c a^2}{\rho_c\pi D} , \quad (29)$$

$$4(\tilde{B}_n - B_n)n(n + 1)\rho_c^{n-1} + 4(\tilde{D}_n - D_n)n(n - 1)\rho_c^{-(n+1)}$$

$$= \frac{a^2 P_c}{\rho_c\pi D} , \quad n \geq 2 . \quad (30)$$

Now we have the complete systems of equations required to express the constants of the inner region in terms of those of the outer region. We will do this for three cases of loading: (1) a point force P_c, (2) a radial moment $M_c\sin\alpha$, and (3) a tangential moment $M_c\cos\alpha$.

3.3. Inner region constants

3.3.1. Case 1: point force P_c

Solving Eqs. (14) through (22) and (28) through (30), we have the following:

For $n = 0$,

$$A_0 = \tilde{A}_0 - \frac{P_c a^2}{8\pi D}\rho_c^2(1 - \ln\rho_c) , \quad (31)$$

$$B_0 = \tilde{B}_0 + \frac{P_c a^2}{8\pi D}(1 + \ln\rho_c) , \quad (32)$$

$$C_0 = \tilde{C}_0 - \frac{P_c a^2}{8\pi D}\rho_c^2 , \quad (33)$$

$$D_0 = \tilde{D}_0 - \frac{P_c a^2}{8\pi D} . \quad (34)$$

For $n = 1$,

$$A_1 = \tilde{A}_1 - \frac{P_c a^2}{16\pi D}4\rho_c\ln\rho_c , \quad (35)$$

$$B_1 = \tilde{B}_1 - \frac{P_c a^2}{16\pi D}\frac{1}{\rho_c} , \quad (36)$$

$$C_1 = \tilde{C}_1 + \frac{P_c a^2}{16\pi D}\rho_c^3 , \quad (37)$$

$$D_1 = \tilde{D}_1 + \frac{P_c a^2}{16\pi D}4\rho_c . \quad (38)$$

For $n \geq 2$,

$$A_n = \tilde{A}_n + \frac{P_c a^2}{8\pi D} \frac{\rho_c^{2-n}}{n(n-1)} , \tag{39}$$

$$B_n = \tilde{B}_n - \frac{P_c a^2}{8\pi D} \frac{\rho_c^{-n}}{n(n+1)} , \tag{40}$$

$$C_n = \tilde{C}_n + \frac{P_c a^2}{8\pi D} \frac{\rho_c^{n+2}}{n(n+1)} , \tag{41}$$

$$D_n = \tilde{D}_n - \frac{P_c a^2}{8\pi D} \frac{\rho_c^{n}}{n(n-1)} . \tag{42}$$

3.3.2. *Case 2: radial moment $M_c \sin\alpha$*

Making the substitution indicated by Eq. (3) into Eqs. (31) through (42), we obtain the formulas for the inner region constants for this case.

For $n = 0$,

$$A_0 = \tilde{A}_0 - \frac{M_c a \sin\alpha}{8\pi D} \rho_c (1 - 2\ln\rho_c) , \tag{43}$$

$$B_0 = \tilde{B}_0 + \frac{M_c a \sin\alpha}{8\pi D} \frac{1}{\rho_c} , \tag{44}$$

$$C_0 = \tilde{C}_0 - \frac{M_c a \sin\alpha}{8\pi D} 2\rho_c , \tag{45}$$

$$D_0 = \tilde{D}_0 . \tag{46}$$

For $n = 1$,

$$A_1 = \tilde{A}_1 - \frac{M_c a \sin\alpha}{16\pi D} 4(1 + \ln\rho_c) , \tag{47}$$

$$B_1 = \tilde{B}_1 + \frac{M_c a \sin\alpha}{16\pi D} \frac{1}{\rho_c^2} , \tag{48}$$

$$C_1 = \tilde{C}_1 + \frac{M_c a \sin\alpha}{16\pi D} 3\rho_c^2 , \tag{49}$$

$$D_1 = \tilde{D}_1 + \frac{M_c a \sin\alpha}{16\pi D} 4 . \tag{50}$$

For $n \geq 2$,

$$A_n = \tilde{A}_n - \frac{M_c a \sin\alpha}{8\pi D} \frac{(n-2)\rho_c^{1-n}}{n(n-1)} , \tag{51}$$

$$B_n = \tilde{B}_n + \frac{M_c a \sin\alpha}{8\pi D} \frac{\rho_c^{-(n+1)}}{n+1} , \tag{52}$$

$$C_n = \tilde{C}_n + \frac{M_c a \sin\alpha}{8\pi D} \frac{(n+2)\rho_c^{n+1}}{n(n+1)} , \tag{53}$$

$$D_n = \tilde{D}_n - \frac{M_c a \sin\alpha}{8\pi D} \frac{\rho_c^{n-1}}{n-1} . \tag{54}$$

It can be shown that substitutions for the integration constants from Eqs. (43) through (54) into the left side of Eqs. (14) through (22) and (28) through (30) yield zeros, except for those corresponding to the continuity condition (15). In this case, since the applied loading is a concentrated radial moment, the results are

$$\frac{M_0 a \sin\alpha}{2\rho_c \pi D} , \quad n = 0 ; \quad \frac{M_0 a \sin\alpha}{\rho_c \pi D} , \quad n \geq 1 .$$

This verifies that the condition of radial moment balance given by

$$\left[M_{r_n} - \tilde{M}_{r_n} \right]_{\rho=\rho_c} = \frac{M_c \sin\alpha}{\rho_c \pi a} \left(\frac{1}{2} + \sum_{n=1}^{\infty} \cos n\phi \right) \tag{55}$$

is satisfied. This is similar to the shear force balance Eq. (24) for the case of a point force. Moreover, as expected, there is no longer a shear force discontinuity at $\rho = \rho_c$.

3.3.3. *Case 3: tangential moment $M_c \cos\alpha$*

The required formulas are obtained by making substitution of Eq. (4) into Eqs. (35) through (42). There are no constants for $n = 0$ because only $\sin n\phi$ terms are allowed.

For $n = 1$,

$$A_1 = \tilde{A}_1 + \frac{M_c a \cos\alpha}{16\pi D} 4(\ln\rho_c) , \tag{56}$$

$$B_1 = \tilde{B}_1 + \frac{M_c a \cos\alpha}{16\pi D} \frac{1}{\rho_c^2} , \tag{57}$$

$$C_1 = \tilde{C}_1 - \frac{M_c a \cos\alpha}{16\pi D} \rho_c^2 , \tag{58}$$

$$D_1 = \tilde{D}_1 - \frac{M_c a \cos\alpha}{16\pi D} 4 . \tag{59}$$

For $n \geq 2$,

$$A_n = \tilde{A}_n - \frac{M_c a \cos\alpha}{8\pi D} \frac{\rho_c^{1-n}}{n-1} , \tag{60}$$

$$B_n = \tilde{B}_n + \frac{M_c a \cos\alpha}{8\pi D} \frac{\rho_c^{-(n+1)}}{n+1} , \tag{61}$$

$$C_n = \tilde{C}_n - \frac{M_c a \cos\alpha}{8\pi D} \frac{\rho_c^{n+1}}{n+1} , \tag{62}$$

$$D_n = \tilde{D}_n + \frac{M_c a \cos\alpha}{8\pi D} \frac{\rho_c^{n-1}}{n-1} . \tag{63}$$

By a substitution for the integration constants from Eqs. (56) through (63) into Eqs. (17) through (22), (29), and (30), it can be shown that the continuity conditions for deflection, slope, and curvature are satisfied, but the applied tangential bending moment causes a shear force discontinuity at $\rho = \rho_c$ equivalent to an applied point force given by

$$\frac{d}{d\phi} \frac{M_c}{c} \cos\alpha . \tag{64}$$

This is equivalent to replacing P_c in Eq. (23) by expression (64).

3.4. Boundary conditions

It now remains to evaluate the outer region constants by means of the boundary conditions—two each for the inner and outer boundaries. First, since there is no central hole in the mirror, we conclude from an examination of expressions (6), (7), and (8) that for keeping the deflection function and its derivatives finite at the center, we must have

$$C_n = D_n = 0 \ , \quad \text{for all } n \geq 0 \ . \tag{65}$$

Next, since the outer boundary is free, the radial moment and the boundary reaction force must vanish at $\rho = 1$. Therefore, for all $n \geq 0$, we have

$$\left[\tilde{M}_{r_n}\right]_{\rho=1} = 0 \ , \tag{66}$$

$$\tilde{V}_{r_n} = \left[\tilde{Q}_{r_n} - \frac{\partial \tilde{M}_{r\iota_n}}{r\partial\phi}\right]_{\rho=1} = 0 \ , \tag{67}$$

where

$$\tilde{M}_{r_n} = -\frac{D}{a^2}\left[(1-\nu)\frac{\partial^2 \tilde{w}_n}{\partial\rho^2} + \nu\nabla^2\tilde{w}_n\right] , \tag{68}$$

$$\tilde{M}_{r\iota_n} = \frac{D}{a^2}(1-\nu)\frac{\partial}{\partial\rho}\left(\frac{1}{\rho}\frac{\partial\tilde{w}_n}{\partial\phi}\right) , \tag{69}$$

and $\tilde{Q}_{r_n}$ is given by a formula similar to Eq. (24). Substitutions from Eqs. (10), (11), and (12) into Eqs. (68) and (69) yield the following equations:

$$2\tilde{B}_0(1+\nu) - \tilde{C}_0(1-\nu) + \tilde{D}_0(3+\nu) = 0 \ , \tag{70}$$

$$\frac{4\tilde{D}_0}{a} = 0 \ , \tag{71}$$

$$2\tilde{B}_1(3+\nu) + 2\tilde{C}_1(1-\nu) + \tilde{D}_1(1+\nu) = 0 \ , \tag{72}$$

$$2\tilde{B}_1(3+\nu) + 2\tilde{C}_1(1-\nu) - \tilde{D}_1(3-\nu) = 0 \ , \tag{73}$$

$$\begin{aligned}&\tilde{A}_n n(n-1)(1-\nu) + \tilde{B}_n(n+1)[(n+2) - \nu(n-2)] \\ &\quad + \tilde{C}_n n(n+1)(1-\nu) + \tilde{D}_n(n-1) \\ &\quad \times [(n-2) - \nu(n+2)] = 0 \ ,\end{aligned} \tag{74}$$

$$\begin{aligned}&\tilde{A}_n n(n-1)(1-\nu) - \tilde{B}_n(n+1)[4 - n(1-\nu)] \\ &\quad - \tilde{C}_n n(n+1)(1-\nu) - \tilde{D}_n(n-1)[4 + n(1-\nu)] = 0 \ .\end{aligned} \tag{75}$$

This completes the set of boundary condition equations required to determine the integration constants for the outer region. As before, we consider three cases of loading. First, we will obtain the formulas for $\tilde{C}_n$ and $\tilde{D}_n$ for the three cases separately and then solve for $\tilde{A}_n$ and $\tilde{B}_n$ in terms of $\tilde{C}_n$ and $\tilde{D}_n$.

3.5. Outer region constants

3.5.1. Case 1: point force P_c

By virtue of Eq. (65), we have the following from Eqs. (33), (34), (37), (38), (41), and (42):

For $n = 0$,

$$\tilde{C}_0 = \frac{P_c a^2}{8\pi D}\rho_c^2 \ , \quad \tilde{D}_0 = \frac{P_c a^2}{8\pi D} \ . \tag{76}$$

For $n = 1$,

$$\tilde{C}_1 = -\frac{P_c a^2}{16\pi D}\rho_c^3 \ , \quad \tilde{D}_1 = -\frac{P_c a^2}{16\pi D}4\rho_c \ . \tag{77}$$

For $n \geq 2$,

$$\tilde{C}_n = -\frac{P_c a^2}{8\pi D}\frac{P_c^{n+2}}{n(n+1)} \ , \quad \tilde{D}_n = \frac{P_c a^2}{8\pi D}\frac{\rho_c^n}{n(n-1)} \ . \tag{78}$$

3.5.2. Case 2: radial moment $M_c \sin\alpha$

By virtue of Eq. (65), Eqs. (45), (46), (49), (50), (53), and (54) yield the following:

For $n = 0$,

$$\tilde{C}_0 = \frac{M_c \sin\alpha}{8\pi D}2\rho_c \ , \quad \tilde{D}_0 = 0 \ , \tag{79}$$

For $n = 1$,

$$\tilde{C}_1 = \frac{M_c a \sin\alpha}{16\pi D}3\rho_c^2 \ , \quad \tilde{D}_1 = -\frac{M_c a \sin\alpha}{16\pi D}4 \ . \tag{80}$$

For $n \geq 2$,

$$\tilde{C}_n = -\frac{M_c a \sin\alpha}{8\pi D}\frac{(n+2)\rho_c^{n+1}}{n(n+1)} \ , \quad \tilde{D}_n = \frac{M_c a \sin\alpha}{8\pi D}\frac{\rho_c^{n-1}}{n-1} \ . \tag{81}$$

3.5.3. Case 3: tangential moment $M_c \cos\alpha$

The required formulas are obtained from Eqs. (58), (59), (62), and (63) by making C_n zero for all n in accordance with Eq. (65). There are no constants corresponding to $n = 0$ because only $\sin n\phi$ terms are involved.

For $n = 1$,

$$\tilde{C}_n = \frac{M_c a \cos\alpha}{16\pi D}\rho_c^2 \ , \quad \tilde{D}_1 = \frac{M_c a \cos\alpha}{16\pi D}4 \ . \tag{82}$$

For $n \geq 2$,

$$\tilde{C}_n = \frac{M_c a \cos\alpha}{16\pi D}\frac{\rho_c^{n+1}}{n+1} \ , \quad \tilde{D}_n = -\frac{M_c a \cos\alpha}{8\pi D}\frac{\rho_c^{n-1}}{n-1} \ . \tag{83}$$

3.5.4. Common to all three cases

Solving Eqs. (70) through (75) for the outer boundary conditions, we obtain formulas that are common to all three types of applied loads under consideration.

For $n = 0$,

$$\tilde{B}_0 = \frac{1-\nu}{2(1+\nu)}\tilde{C}_0 \ , \quad \tilde{D}_0 = 0 \ . \tag{84}$$

For $n = 1$,

$$\tilde{B}_1 = -\frac{1-\nu}{3+\nu}\tilde{C}_1 \ , \quad \tilde{D}_1 = 0 \ . \tag{85}$$

For $n \geq 2$,

$$\tilde{A}_n = \frac{n(n+1)(1-\nu)^2\tilde{C}_n + [n^2(1-\nu)^2 + 8(1+\nu)]\tilde{D}_n}{n(1-\nu)(3+\nu)}, \quad (86)$$

$$\tilde{B}_n = -\frac{(1-\nu)[n\tilde{C}_n + (n-1)\tilde{D}_n]}{3+\nu}. \quad (87)$$

3.6. Comments

This formally completes the derivation of the moment actuator influence function. Since $\tilde{C}_n$ and $\tilde{D}_n$ are given by Eqs. (76) through (83), $\tilde{A}_n$ and $\tilde{B}_n$ for all values of n can be computed from Eqs. (84) through (87) except $\tilde{A}_0$ and $\tilde{A}_1$. However, these two constants merely define the rigid body piston and tilt components of motion and can be ignored.

It now remains to resolve an apparent contradiction in the formulas for $\tilde{D}_0$ and $\tilde{D}_1$ obtained from the inner and outer boundary conditions. These two constants are zero according to the second formulas in Eqs. (84) and (85), obtained from the condition of free outer boundary. With the exception of the second formula in Eq. (79) for $\tilde{D}_0$ in the case of applied radial moment, this does not agree with the corresponding expressions obtained from the inner boundary and continuity conditions as evidenced in the second formulas in Eqs. (76), (77), (80), and (82). Any of the three types of applied load would, by itself acting alone, result in nonzero or unbalanced radial moment and transverse reaction force at the outer boundary. However, in our application, there is always a system of two statically balanced moments applied at the actuator post locations A and B (Fig. 2). Further, the case of point force is never used, except for approximating a moment with two equal and opposite forces a small distance $2c$ apart so that $M_0 = 2P_c c$, when either post A or B coincides with the center of the mirror. In this type of application, it is automatically ensured that the net radial moment and shear force due to a moment actuator are zero at the outer boundary. In general, this is true for any statically balanced system of applied moments.

3.6.1. *Support deflection*

Two types of support options are provided with this solution. The mirror may be either kinematically supported on three points at radius $\rho = \rho_s$ or fixed at the center. Denoting the support point deflections by w_{s1}, w_{s2}, and w_{s3}, in the case of a three-point support, the ensuing rigid body piston and tilt components of motion can be easily calculated.[3] For the case of a fixed-center support, the rigid body piston and tilt simply correspond to the deflection and slope of the center. The datum plane of deflection is obtained by subtracting the above rigid body effects from the gross deflection of the mirror.

4. ILLUSTRATIVE NUMERICAL RESULTS

For the convenience of making rapid calculations, the formulas of the above closed form solution for the influence function of a moment actuator were embodied into a FORTRAN routine and the influence functions were computed for a number of test cases, identified in Table II. The assumed mirror configuration is shown in Table III. Contour plots of these influence functions are presented in Fig. 5. The plots for the three-point supports

TABLE II. Case matrix of test runs.

Case No.	Type of Moment	Actuator Location A	Actuator Location B
1	Radial	0°	1°
2	Radial	1°	2°
3	Radial	2°	3°
4	Tangential	0°	1°
5	Tangential	1°	2°
6	Tangential	2°	3°

TABLE III. Assumed mirror configuration for the test runs.

Mirror diameter	= 6.0 inches
Mirror thickness	= 3/16 inch
Young's modulus	= 10 x 10^6 psi
Poisson's ratio	= 0.33
Support types:	3-point at r = 2 inches and fixed center

are on the left side and those for the central supports are on the right. Rigid body piston and tilt effects constitute the only difference between the two plots. Additionally, a 61 μrad tilt about the y axis has been subtracted from the computed data in the right contour plot of Fig. 5(a). The plots illustrate the global character of these influence functions.

Since a detailed finite element model was planned for the detailed design stage incorporating all important design details, which were to be ignored in the closed form solution based configuration trade-off analysis, it was of some interest to see how well the results of these two different approaches would correlate under the same set of simplifying assumptions. Accordingly, influence functions for the same matrix of test runs were also computed using a Nastran based finite element model of the above mirror configuration, using quadrilateral (QUAD4) and triangular (TRIA3) plate elements and excluding the expected design details. The results for the six test cases are compared in the diametral and/or boundary deflection profiles of Fig. 6. The top graph of each part is for the three-point support at $r = 2$ in., while the bottom graph is for the fixed-center support. The difference between the two consists entirely of a rigid body piston and tilt effect. Also included in each figure is the location of the actuator (with ends A and B) and the type of applied moment. The agreement between the closed form and Nastran solutions is excellent in all cases.

5. CONCLUSION

With development of a closed form derivation of the moment actuator influence function, the stage is now set for performing configurational trade-off analyses for the development of a near-optimum circular deformable mirror with diametral arrays of radial moment actuators. This trade-off approach is significantly more cost-effective, both in man-hours and computational time, compared to a finite element approach. Consequently, a finite

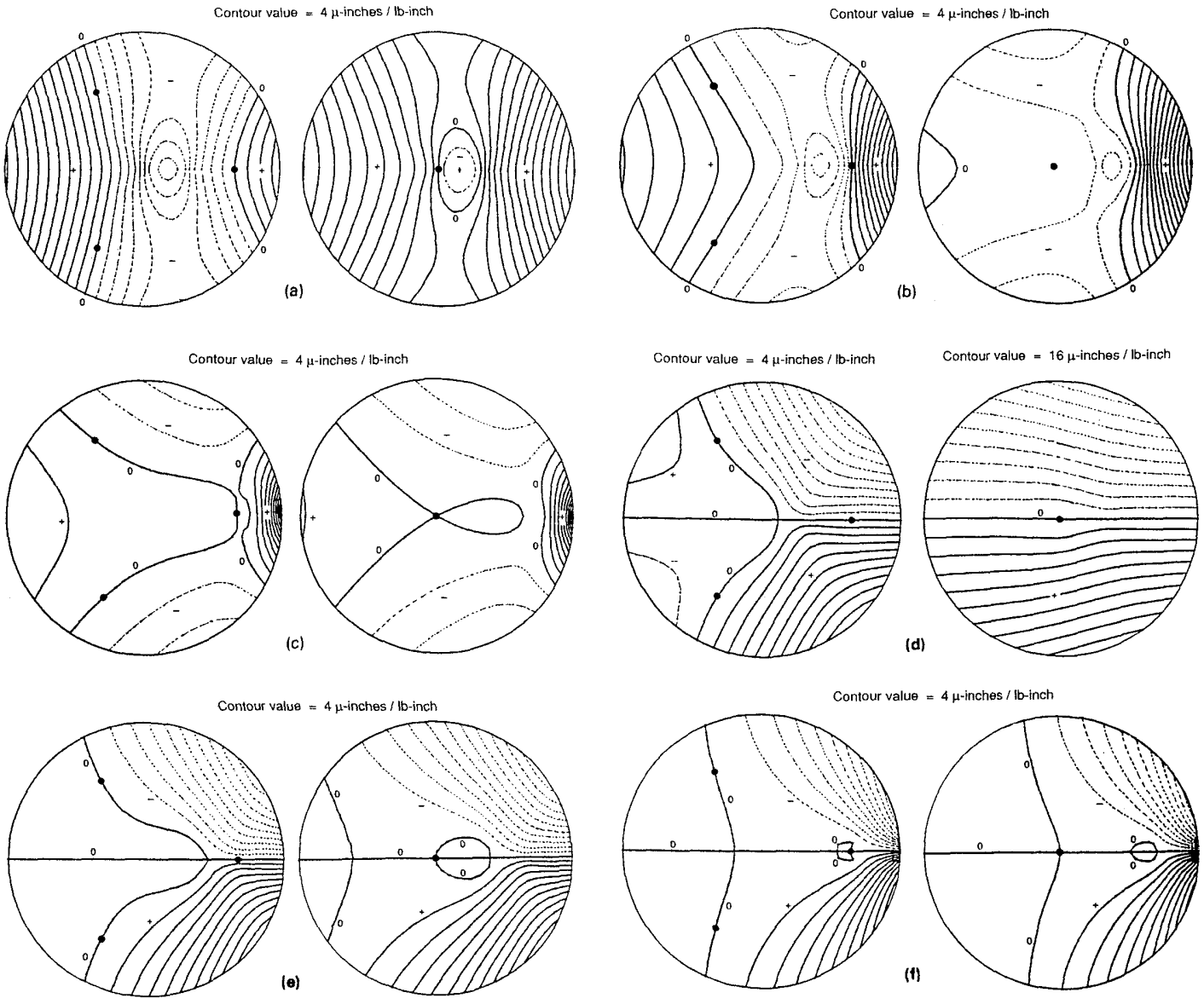

Fig. 5. Influence function contour plots for three-point (left) and central (right) supports. (The supports are indicated by the bold dots.) (a) Case 1: radial moment actuator between $\rho = 0$ and $\rho = 1/3$. (b) Case 2: radial moment actuator between $\rho = 1/3$ and $\rho = 2/3$. (c) Case 3: radial moment actuator between $\rho = 2/3$ and $\rho = 1$. (d) Case 4: tangential moment actuator between $\rho = 0$ and $\rho = 1/3$. (e) Case 5: tangential moment actuator between $\rho = 1/3$ and $\rho = 2/3$. (f) Case 6: tangential moment actuator between $\rho = 2/3$ and $\rho = 1$.

element model (FEM) is not needed until the detailed design stage. Further, any deviation in performance prediction based on a detailed FEM analysis is solely due to the effects of configuration details included in the finite element model and not due to a different analytical approach (closed form solution) used in the trade-off and configuration development stage. It was shown in the comparative data presented in the final report[1] on the project that the design details, ignored in the closed form analysis and included in the finite element model, had negligible effect on the results.

An application of this approach along with detailed design and analysis, test results, successful correlation between tests and analysis, the correction capability of the mirror, etc. were planned to be reported in a companion paper. This paper had to be withdrawn from publication due to customer's disapproval for a public release of this information. However, the information is available in an unclassified final report[1] on the project. Under the circumstances, it suffices to say that excellent correlation was achieved between the predicted performance and measurements.

6. ACKNOWLEDGMENT

The work leading to this paper was performed under contract F-30602-87-C-0195 for the Space Communication Branch of Rome Air Development Center, Griffiss AFB, New York.

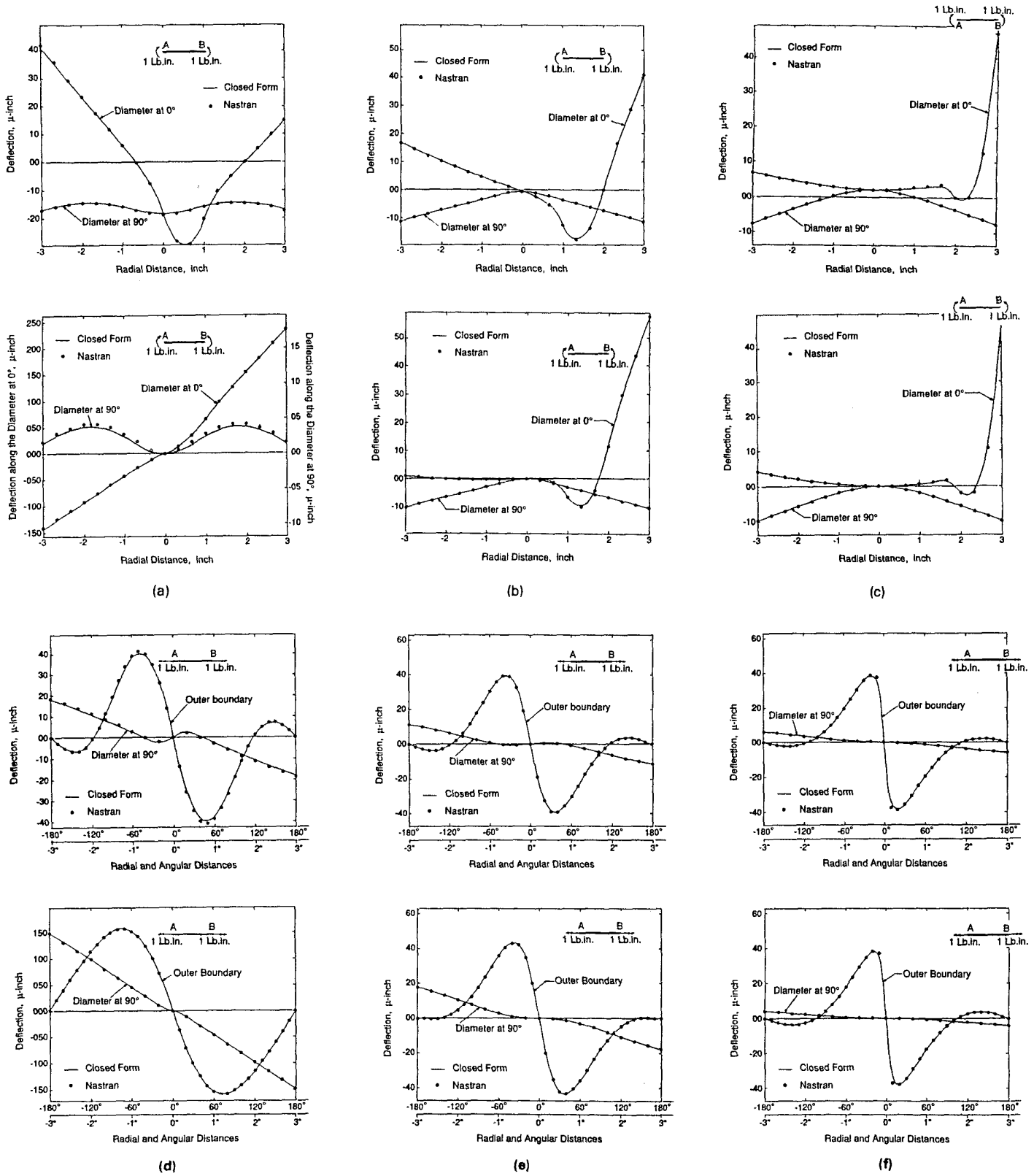

Fig. 6. Correlation between the closed form and Nastran solutions for three-point support at $r = 2$ in. (top graphs) and central supports (bottom graphs). (a) Case 1: radial moment actuator between $\rho = 0$ and $\rho = 1/3$. (b) Case 2: radial moment actuator between $\rho = 1/3$ and $\rho = 2/3$. (c) Case 3: radial moment actuator between $\rho = 2/3$ and $\rho = 1$. (d) Case 4: tangential moment actuator between $\rho = 0$ and $\rho = 1/3$. (e) Case 5: tangential moment actuator between $\rho = 1/3$ and $\rho = 2/3$. (f) Case 6: tangential moment actuator between $\rho = 2/3$ and $\rho = 1$.

7. REFERENCES

1. P. K. Mehta, D. H. Kittel, and M. E. Haller, "System wavefront corrector," Final Rept. F30602-87-C-0195 (unclassified), C. Roychoudhuri, program manager, prepared by Perkin-Elmer Corp. for RADC, Griffiss AFB, Rome, NY 13441 (March 1989).
2. S. Timoshenko and S. Woinowsky-Krieger, *Theory of Plates and Shells*, pp. 290–291, McGraw-Hill Book Company, Inc., 2nd. edition (1959).
3. P. K. Mehta, "Nonsymmetric Thermal Bowing of Curved Circular Mirrors," in *Structural Mechanics II*, Alson E. Hatheway, ed., Proc. SPIE 748, 193–194 (1987).

Pravin K. Mehta received the B.Sc. degree in mathematics from the University of Bombay, India, in 1957 and the DMIT degree in aeronautical engineering from the Madras Institute of Technology, India, in 1960. He received the MS and Ph.D. degrees in engineering mechanics from the Pennsylvania State University in 1962 and 1966, respectively. After spending a year on the Penn State faculty as an assistant professor in 1966–67, he joined the Electro-Optical Division of Perkin-Elmer Corp. in 1967. This division, after a recent acquisition by Hughes Aircraft Co., now operates as Hughes Danbury Optical Systems, Inc., where he is currently a senior scientist in systems engineering. He has published papers on a variety of subjects in engineering mechanics and optostructural mechanics. He is a founding member of the American Academy of Mechanics.